NAVAL POSTGRADUATE SCHOOL

MONTEREY, CALIFORNIA

THESIS

PERFORMANCE OF A LIQUID FLOW ULTRA-COMPACT HEAT EXCHANGER

by

Michael A. Sammataro

June 2006

Thesis Advisor:	Ashok Gopinath
Second Reader:	Jose Sinibaldi

Approved for public release; distribution is unlimited

THIS PAGE INTENTIONALLY LEFT BLANK

REPORT DOCUMENTATION PAGE			Form Approved OMB No. 0704-0188
Public reporting burden for this collection of information is estimated to average 1 hour per response, including the time for reviewing instruction, searching existing data sources, gathering and maintaining the data needed, and completing and reviewing the collection of information. Send comments regarding this burden estimate or any other aspect of this collection of information, including suggestions for reducing this burden, to Washington headquarters Services, Directorate for Information Operations and Reports, 1215 Jefferson Davis Highway, Suite 1204, Arlington, VA 22202-4302, and to the Office of Management and Budget, Paperwork Reduction Project (0704-0188) Washington DC 20503.			
1. AGENCY USE ONLY ***(Leave blank)***	**2. REPORT DATE** June 2006	**3. REPORT TYPE AND DATES COVERED** Master's Thesis	
4. TITLE AND SUBTITLE Performance of a Liquid Flow Ultra-Compact Heat Exchanger		**5. FUNDING NUMBERS**	
6. AUTHOR(S) Michael A. Sammataro			
7. PERFORMING ORGANIZATION NAME(S) AND ADDRESS(ES) Naval Postgraduate School Monterey, CA 93943-5000		**8. PERFORMING ORGANIZATION REPORT NUMBER**	
9. SPONSORING /MONITORING AGENCY NAME(S) AND ADDRESS(ES) N/A		**10. SPONSORING/MONITORING AGENCY REPORT NUMBER**	
11. SUPPLEMENTARY NOTES The views expressed in this thesis are those of the author and do not reflect the official policy or position of the Department of Defense or the U.S. Government.			
12a. DISTRIBUTION / AVAILABILITY STATEMENT **Approved for public release; distribution is unlimited**		**12b. DISTRIBUTION CODE** A	

13. ABSTRACT (maximum 200 words)

A numerical analysis of the performance of compact pin-fin array heat exchangers was carried out using water and JP-4 fuel as the working fluids. Three different configurations were used with hydraulic diameters ranging from 0.137 to 0.777 mm, and volumetric area densities varying between 4.5 and 14.5 mm^2/mm^3. Numerical simulations were carried out to determine the performance of each heat exchanger over a series of Reynolds numbers in both the laminar and turbulent flow regimes. It was found that very large heat transfer coefficients (in the kW/m^2K range) can be achieved compared to air for the same footprint. In addition, the simulations were used to predict the Reynolds number range for transition from laminar to turbulent flow which was found to vary depending on the compactness of the heat exchanger configuration. As a final point, this study also investigated the effects of boiling of the liquid within the heat exchanger on its performance. It was found that despite improved heat transfer rates due to latent heat removal, vapor formation and resulting fluid expansion effects could result in undesirable flow patterns at low Reynolds numbers. The results from this study would be useful in the design of micro-scale heat exchangers for applications in the micro-electronic and gas turbine industries.

14. SUBJECT TERMS Pin Fin Array, Heat Exchanger, Micro Scale, Computational Fluid Dynamics, Laminar, Turbulent			**15. NUMBER OF PAGES** 65
			16. PRICE CODE
17. SECURITY CLASSIFICATION OF REPORT Unclassified	**18. SECURITY CLASSIFICATION OF THIS PAGE** Unclassified	**19. SECURITY CLASSIFICATION OF ABSTRACT** Unclassified	**20. LIMITATION OF ABSTRACT** UL

NSN 7540-01-280-5500

Standard Form 298 (Rev. 2-89)
Prescribed by ANSI Std. 239-18

THIS PAGE INTENTIONALLY LEFT BLANK

Approved for public release; distribution is unlimited

PERFORMANCE OF A LIQUID FLOW ULTRA-COMPACT HEAT EXCHANGER

Michael A. Sammataro
Ensign, United States Navy
B.S., United States Naval Academy, 2005

Submitted in partial fulfillment of the
requirements for the degree of

MASTER OF SCIENCE IN MECHANICAL ENGINEERING

from the

NAVAL POSTGRADUATE SCHOOL
JUNE 2006

Author: Michael A. Sammataro

Approved by: Ashok Gopinath
Thesis Advisor

Jose Sinibaldi
Second Reader/Co-Advisor

Anthony J. Healey
Chairman, Department of Mechanical Engineering

THIS PAGE INTENTIONALLY LEFT BLANK

ABSTRACT

A numerical analysis of the performance of compact pin-fin array heat exchangers was carried out using water and JP-4 fuel as the working fluids. Three different configurations were used with hydraulic diameters ranging from 0.137 to 0.777 mm, and volumetric area densities varying between 4.5 and 14.5 mm^2/mm^3. Numerical simulations were carried out to determine the performance of each heat exchanger over a series of Reynolds numbers in both the laminar and turbulent flow regimes. It was found that very large heat transfer coefficients (in the kW/m^2K range) can be achieved compared to air for the same footprint. In addition, the simulations were used to predict the Reynolds number range for transition from laminar to turbulent flow which was found to vary depending on the compactness of the heat exchanger configuration. As a final point, this study also investigated the effects of boiling of the liquid within the heat exchanger on its performance. It was found that despite improved heat transfer rates due to latent heat removal, vapor formation and resulting fluid expansion effects could result in undesirable flow patterns at low Reynolds numbers. The results from this study would be useful in the design of micro-scale heat exchangers for applications in the micro-electronic and gas turbine industries.

THIS PAGE INTENTIONALLY LEFT BLANK

TABLE OF CONTENTS

LIST OF FIGURES

THIS PAGE INTENTIONALLY LEFT BLANK

LIST OF TABLES

NOMENCLATURE

A	Area [m^2]
$A_{array,ave}$	Average Array Flow Area [m^2]
A_{wetted}	Wetted Internal Area of Array [m^2]
C_p	Specific Heat [J/kg*K]
D	Pin Diameter [m]
D_h	Hydraulic Diameter [m]
ε	Effectiveness
H	Heat Exchanger Height [m]
$h_{array,ave}$	Average Heat Transfer Coefficient [W/m^2*K]
k	Conductivity [W/m*K]
NTU	Number of Transfer Units
N_s	Number of Spans
N_x	Number of Cell Lengths
ΔQ	Change in Heat Rate [W]
Q_{in}	Inlet Heat Rate [W]
Q_{out}	Outlet Heat Rate [W]
q	Heat Flux [W/m^2]
q_{max}	Maximum Heat Flux [W/m^2]
Re_{Dh}	Reynolds Number based on Hydraulic Diameter
S	Unit Cell Span [m]
ΔT_{lm}	Log-Mean Temperature Difference [K]
$T_{bulk,out}$	Bulk Outlet Temperature [K]
T_{in}	Inlet Temperature [K]
T_{wall}	Wall Temperature [K]
u	Velocity in the x direction [m/s]
U_{max}	Maximum (centerline) velocity in the x direction [m/s]
V_{in}	Average inlet velocity [m/s]
X	Unit Cell Length [m]
z	Height from the baseline of the heat exchanger [m]

THIS PAGE INTENTIONALLY LEFT BLANK

AKNOWLEDGEMENTS

I would like to thank Professor Gopinath for finding me a project to work on after my initial thesis project was delayed, and for having the patience to walk me through some of the concepts more than once.

I would also like to thank Professor Sinibaldi, who started my interest in the field of heat transfer while I was in his class, and who made sure that I understood the basics.

Finally, I would like to thank Jessica, my wonderful wife, who helped me stay sane while I was working on this project, and kept me from getting *too* angry when my simulations didn't converge.

THIS PAGE INTENTIONALLY LEFT BLANK

I. INTRODUCTION

A. BACKGROUND

High performance is the standard of success for the modern engineer. Computer systems must run faster, cooler, and more efficiently. Likewise, turbine engines are pushed to achieve higher efficiency and greater levels of output power. The common thread in both of these applications is that higher performance results in higher operating temperatures. Given the scale of operation in both cases, the use of micro-heat exchangers to improve system performance is essential.

To date, the common working fluid in these systems has been air. However, as research in micro electro-mechanical systems (MEMS) has progressed, the technology has become available to miniaturize the various mechanical systems necessary to pump water or other working fluids through these systems. The obvious attraction to do so is the higher heat transfer rates that can be achieved with fluids other than air.

1. Computer Industry

The current generation of computer processors is largely air-cooled, relying on the use of fans and bulky pin-fin arrays to facilitate heat transfer from the processor (see Figure 1). The attraction of using a more efficient heat exchanger is in the higher performance (processing speed) that can be achieved if the processor is more quickly and effectively cooled.

Adding a water-cooled micro-scale heat exchanger to a computer offers many benefits. Fans and large internal and external heat sinks would be eliminated in favor of a relatively small pump and water reservoir. This in turn would reduce the power draw from a given computer system, as well as increasing processing speed.

Figure 1. A common forced-convection computer processor heat sink (Furukawa America)

2. Gas Turbine Industry

As turbine inlet temperature increases, so does its performance. Likewise, as temperature increases, so does wear on the blades. Over the life of the turbine, this fatigue of the blades can lead to highly degraded performance. Dimas (2005) The gas turbine industry currently uses ventilated blades, with various designs and arrays of tubes to allow the circulation of air through the blade to cool it (see Figures 2-3). Using the simply ventilated blade described above caps the heat transfer rate, which along with the properties of the blade materials, limits the temperatures the blade can be exposed to, and therefore the overall performance of the turbine.

The addition of a micro-scale heat exchanger to such a system would be a great benefit to the turbine designer. The ability to use a working fluid other than air would greatly increase the heat transfer rate. The use of water, however, would involve adding more machinery, albeit small machinery, to the turbine. In an industry where size and weight matter greatly, other options must be considered. This is where the use of fuel as the working fluid comes into play.

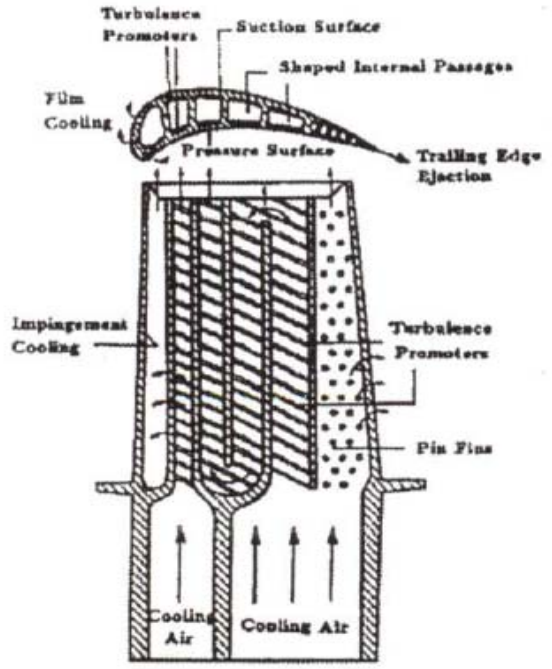

Figure 2. Turbine blade internal cooling passage (Dimas 2005)

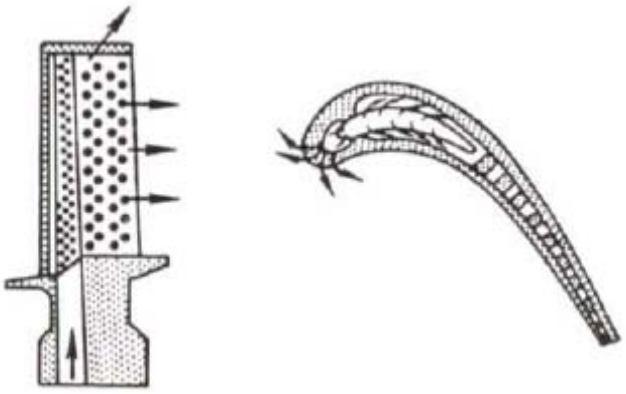

Figure 3. Cooled turbine airfoil with pin fins (Metzger 1984)

Using fuel in the turbine blade heat exchangers offers several benefits, the first of which is the elimination of extra tanks and pumps necessary for the introduction of a separate working fluid. Another advantage would come from pre-heating the fuel before it is introduced to the combustor. Obviously, this is also cause for skepticism; the danger of premature combustion of the fuel (and therefore destruction of the engine) is one major drawback of this concept.

B. OBJECTIVES

1. Laminar to Turbulent Transition

The purpose of this study is to find methods to make micro heat exchangers more effective. Accordingly, a study of laminar versus turbulent flow is necessary to find the most efficient means of heat transfer. CFD-ACE allows for the inclusion of turbulent effects. However, a chief concern at the beginning of this study was that ACE would seemingly "activate" turbulent effects at the commonly accepted Reynolds number of 2300, the approximate transition value for internal flows. This study aims to dispel that idea and show an actual range of values for transition for each heat exchanger.

The transition range will be proven by the effect of turbulence on the Nusselt number for a given Reynolds number. Convective heat transfer theory shows that heat transfer rates for turbulent flows are higher than laminar flows due to the mixing effects caused by the turbulence. Accordingly, this mixing allows for increased heat transfer from the walls of the heat exchanger to the fluid. By performing both laminar and turbulent tests over a given range of Reynolds numbers, the transition to turbulent flow will be proven by finding the range of Reynolds numbers over which the Nusselt number begins increasing.

Because of its effects on heat transfer, turbulent flow is an attractive way to increase the overall performance of a micro heat exchanger. The one downside to turbulence is the increased wear on the internal surfaces of the heat exchanger itself which could, over time, lead to a decrease in system performance.

2. Advantages of Water and JP-4 over Air

Dimas completed a study in this field using air as the working fluid. While air provides reasonably good heat transfer, some applications call for a more effective working fluid.

Water has greater heat transfer capacity than air, and through the Nusselt number and heat transfer coefficients calculated from these simulations, that fact will be proven.

JP-4 similarly has a greater heat transfer capacity than air. Through simulation, it will be shown that it is feasible to use a fuel as a working fluid in a heat exchanger. The benefit of this is not only cooler engine operation, but also the pre-heating of the fuel in the engine.

3. The Effect of Boiling on Heat Exchanger Performance

A major concern for water-cooled heat exchangers in high-temperature applications (at or around the boiling point of water) is that the possibility of a temperature spike could cause the water to boil off through the heat exchanger. While this is welcome in some applications (refrigeration), it is not entirely certain what its effect upon a micro-scale heat exchanger would be. The increased mixing of steam could possibly lead to an increase in heat transfer rate. However, the rapid expansion of water going from liquid to gaseous state may also cause blockage and unfavorable recirculation within the heat exchanger.

Using the Two-Fluid module in CFD-ACE, the phase change of water going from liquid to gaseous state will be simulated. The effects of this change will be analyzed to see if positive or negative effects to the heat transfer rate are incurred.

C. THEORY AND CALCULATIONS

1. Heat Exchanger Parameters and Calculations

The three heat exchangers used for this experiment are of a similar configuration. A general model of the heat exchangers in use, with the proper nomenclature, is shown in Figure 4.

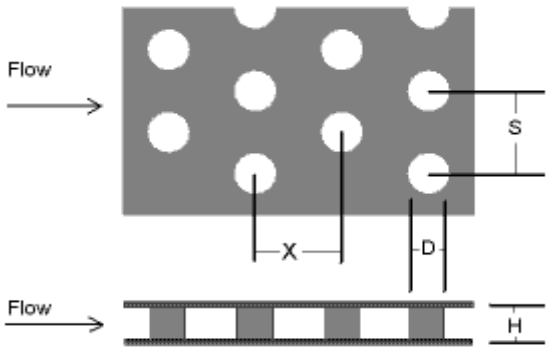

Figure 4. Generalized Heat Exchanger (Choo 2003)

To calculate the Reynolds and Nusselt numbers for each heat exchanger, it is essential to know the hydraulic diameter. This parameter is the length scale which will be used for most of the calculations of heat transfer and flow rate. The hydraulic diameter is calculated as follows.

$$D_h = \frac{4V_{open}}{A_{wetted}} \qquad [m] \qquad (1)$$

The open volume within the heat exchanger itself is the volume of the pins subtracted from the total internal volume, and is given below.

$$V_{open} = N_s \cdot N_x \cdot \left[(X \cdot S \cdot H) - \pi \left(\frac{D^2 \cdot H}{4} \right) \right] \qquad [m^3] \qquad (2)$$

The wetted surface area within the heat exchanger is calculated as follows:

$$A_{wetted} = N_s \cdot N_x \cdot \left[(2 \cdot X \cdot S) - 2\pi \left(\frac{D^2}{4} \right) + \pi (D \cdot H) \right] \qquad [m^2] \qquad (3)$$

The area density of the heat exchanger, a measure of the wetted surface area available per unit volume, is an important parameter when dealing with heat transfer at micro-scale levels.

$$AreaDensity = \frac{A_{wetted}}{1000 L \cdot W \cdot H} \qquad [mm^{-1}] \qquad (4)$$

The average array cross-sectional area is a useful parameter for flow calculations, and is equal to the following.

$$A_{array,avg} = \frac{V_{open}}{L} \qquad \left[m^2 \right] \qquad (5)$$

2. Flow Theory and Calculations

For these simulations, a fully-developed Poiseiulle velocity profile is used as the input boundary condition in CFD. The equations for this profile, as given by White (1999), are as follows.

$$u = u_{\max}\left(1 - \frac{z^2}{H^2}\right) \qquad \left[\frac{m}{s} \right] \qquad (6)$$

The maximum centerline velocity, with respect to the vertical axis, is given as a function of the average inlet velocity.

$$u_{\max} = 1.5 V_{in} \qquad \left[\frac{m}{s} \right] \qquad (7)$$

The experiments conducted for this study are characterized by the Reynolds numbers of the flow through the heat exchangers. Because CFD output includes mass flow rate, it is useful to characterize the flow in terms of that parameter.

$$\mathrm{Re}_{Dh} = \frac{\dot{m} D_h}{\mu A_{array,avg}} \qquad (8)$$

3. Heat Transfer Theory and Calculations

The effectiveness of each heat exchanger in the various flow regimes and working fluids will be characterized by the Nusselt number, a measure of the heat transfer coefficient.

$$Nu = \frac{h_{array,ave} D_h}{k} \tag{9}$$

The average heat transfer coefficient, in W/m2 over the array (of pin-fins in a given heat exchanger) is given as follows:

$$h_{array,ave} = \frac{\Delta Q}{A_{wetted} \Delta T_{lm}} \qquad \left[\frac{W}{m^2 \cdot K}\right] \tag{10}$$

The heat flux over the array, which is to be measured from the CFD output file, is given by:

$$\Delta Q = \left| Q_{in} + Q_{out} \right| \qquad \left[\frac{W}{m^2}\right] \tag{11}$$

The log-mean temperature difference will be used in the calculation of the average heat transfer coefficient, and is given as follows:

$$\Delta T_{lm} = \left[\frac{\left(T_{wall} - T_{in}\right) - \left(T_{wall} - T_{bulk,out}\right)}{\ln\left[\frac{\left(T_{wall} - T_{in}\right)}{\left(T_{wall} - T_{bulk,out}\right)}\right]} \right] \qquad [K] \tag{12}$$

Note that the bulk outlet temperature is an area- and velocity-weighted average to account for the temperature profile of the fluid flow, as well as the cross-sectional area of the outlet.

One more measurement of heat transfer will be used to check the results of the simulation, that of the effectiveness-number of transfer units (NTU) method. The equations for this method are put forth by Incropera and DeWitt (1996). The effectiveness, which is the actual heat transfer rate versus the maximum heat transfer rate, is given by the simplified form:

$$\varepsilon = \frac{q}{q_{\max}} = \frac{T_{out} - T_{in}}{T_{wall} - T_{in}} \tag{13}$$

The number of transfer units (NTU) is given as follows:

$$NTU = \frac{UA}{C_{\min}} = \frac{h_{array,ave} A_{wetted}}{\dot{m} C_p} \tag{14}$$

Effectiveness and the number of transfer units are related by:

$$1 - \varepsilon = e^{-NTU} \tag{15}$$

The numerically calculated values from each simulation will be plotted against this relationship to verify the accuracy of the results.

THIS PAGE INTENTIONALLY LEFT BLANK

II. NUMERICAL SETUP

A. TEST MATRIX

1. Heat Exchanger Configurations

Three different heat exchanger configurations, all using a pin-fin design, were used in this investigation to give a good range of results. The dimensions of each heat exchanger tested are given below in Tables 1 and 2.

	X (m)	D (m)	H (m)	S (m)	L (m)	W (m)	N_x	N_s
HX 3	0.000625	0.000500	0.000405	0.000625	0.002500	0.001250	4	2
HX 7	0.000208	0.000167	0.000405	0.000208	0.000833	0.000417	4	2
HX 9	0.001250	0.000500	0.000500	0.001250	0.007500	0.002500	6	2

Table 1. Basic Heat Exchanger Parameters

	A_{wetted} (m^2)	$V_{open,array}$ (m^3)	D_h (m)	$A_{array,avg}$ (m^2)	Area Density (mm^{-1})	αH
HX 3	8.1978E-06	6.2945E-10	0.000307	2.5178E-07	6.477	2.62
HX 7	2.0418E-06	6.9939E-11	0.000137	8.3927E-08	14.520	5.88
HX 9	4.2212E-05	8.1969E-09	0.000777	1.0929E-06	4.503	2.25

Table 2. Calculated Heat Exchanger Parameters

The heat exchangers chosen for this study offer a variety of sizes, and more importantly, a range of area densities. This factor should prove to be important not only to heat transfer rate, but also to flow conditions within the heat exchanger.

2. Working Fluids and Properties

a. Water

For the simulations with water as the working fluid, the inlet temperature will be 300 K, and the wall temperature will be 320 K (HX 3 and HX 7) or 312 K (HX 9). For all simulations, water properties are evaluated at a film temperature of 310 K. To verify the accuracy of using constant properties, several simulations were run with properties that varied with temperature, and with properties evaluated at different film temperatures. The

results yielded such a small difference as to be negligible. It was therefore judged that for the small range of temperatures evaluated for this study, properties could be assumed constant.

b. JP-4

JP-4 is a common fuel used for gas turbine engines, and is therefore the fuel of choice for the purposes of this study. Since the inlet and wall temperatures are the same was the water experiments, all properties of JP-4 are analyzed at a film temperature of 310 K. The rationale for using constant properties is the same.

c. Water and Steam

For the boiling simulations, the water inlet temperature ranged from 360 to 370 K, with the heat exchanger walls temperatures between 380 of 400 K. This allowed for the analysis of a wide range of conditions that lead to a phase change. Since CFD requires separate inputs for the two phases of water, liquid water properties were evaluated at a film temperature of 370 K. Steam properties were evaluated at 373 K and 101.325 kPa.

3. Reynolds Number Range

This study aims to encompass not only the effects of both laminar and turbulent flows, but also to show the transition. Accordingly, eight Reynolds numbers will be tested for each case: 100, 300, 500, 1000, 2000, 3000, 5000, and 10000. The first three Reynolds numbers show the purely laminar range, with the middle three showing the transitional range, and the final three representing the low-end range of turbulence.

B. COMPUTATIONAL FLUID DYNAMICS (CFD) INPUT

The program CFD-ACE was used to perform the numerical simulations for this project. The models of each heat exchanger were built previously by Sotirios Dimas using CFD-GEOM. A half-model of each heat exchanger, split along its horizontal symmetry plane, was used for each simulation. Figure 5 shows a model of a single cell from within a heat exchanger model, illustrating the prismatic triangular elements used in its construction.

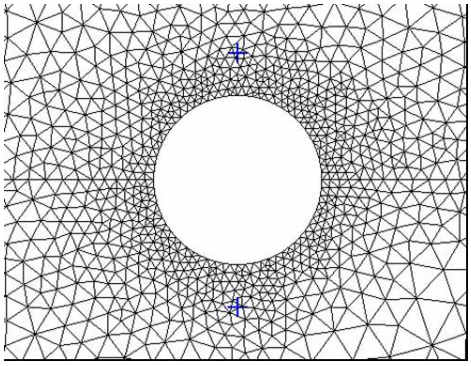

Figure 5. Single cell from a CFD-GEOM Heat Exchanger Model (Dimas 2005)

For the basic problem of water flow through a heat exchanger, laminar and turbulent tests were conducted to find not only the benefits of each type of flow, but also to see if the transition point of theory (Re ≈ 2300) could be approximated using CFD simulations. It is necessary to note that most of the CFD settings applied were kept similar to or the same as the tests performed by Dimas to provide consistency and allow for comparison of the data.

1. Laminar Testing

The initial tests performed were laminar tests of water through each heat exchanger. The water entered the heat exchanger at a constant temperature of 300 K, and the heat exchanger walls were set at an initial temperature of 320 K (or 312 K, in the case of heat exchanger 9). To understand how each test was conducted, a step-by-step procedure of the modules and variables used in the CFD-ACE simulations are listed below.

a. Problem Type

CFD-ACE allows for the activation of various modules to simulate certain problem types. For this simulation, both the Flow and Heat Transfer modules were used. The selection of these modules subsequently activates various tabs and options that are described further in the following sections.

b. Model Options

Under the model options tab on the ‘Shared’ menu, the problem type is kept as steady-state, as the heat exchanger models account for developing flow and other time-dependent factors. On the ‘Flow’ menu, the reference pressure is set at standard atmospheric pressure, 101.325 kPa.

c. Volume Conditions

The volume conditions tab allows for the input of the fluid properties. For the water tests, the ‘Fluid Subtype’ field is set to liquid, and the density, kinematic viscosity, specific heat, and thermal conductivity are all set to constant values evaluated at T_{film} = 310 K.

d. Boundary Conditions

Boundary conditions were set based upon the type of each component in the GEOM model. Since the model built in GEOM is only a half-model, split along the z-axis, a symmetry boundary exists in ACE. All symmetry plane boundaries were set as such, allowing the simulation to run as if there was a continuous volume of fluid with no symmetry plane bisecting it.

Interface boundaries are typical parts of the GEOM construct that exist to help in the building of the model, but are not part of the simulation, and are not part of the actual model. Setting these as interfaces allows ACE to essentially ignore these boundaries, and treat them as a continuous fluid volume.

The inlet to the heat exchanger was set at a constant pressure and temperature of zero kPa and 300 K, respectively. The velocity profile discussed in Chapter II was used to specify the inlet x-direction velocity. The y- and z-direction velocities were set to zero, as all flow entering the model is assumed to be in the x-direction.

The walls of the heat exchanger were set to be isothermal at a constant temperature of 320 K, with no-slip conditions on the wall.

The entry and exit wall of the heat exchanger were set to be adiabatic. This was mainly set as such for the purpose of the numerical analysis, so that the heat transfer was isolated within the heat exchanger.

e. Initial Conditions

This tab allows the user to input the values used for the first iteration of the ACE solution. The temperature was set to a constant 300 K, and the average value of velocity, V_{in}, was entered for the x-direction velocity. Other velocities, as well as the pressure, were all set to zero.

f. Solver Controls

The solver controls were left at their default values for heat exchangers three and nine. The maximum number of iterations was 1500. For heat exchanger seven, the inertial and linear relaxation was increased, due to the area density of that model. The maximum number of iterations was increased to 3000.

g. Output

This tab allows the user to select the values tabulated on in the ACE output file.

2. Turbulent Testing

The turbulent simulation setup was very similar to the laminar setup. Therefore, only the additional modules and controls that were activated for the turbulent problem are listed.

a. Problem Type

The turbulence module was selected, activating the subsequent modifications listed and allowing for the simulation of the transition to turbulence.

b. Model Options

From the turbulence tab of this menu, the K-ε model of turbulence was selected. The default turbulent Prandtl number of 0.9 was kept for this simulation, as well as the standard wall function.

c. Boundary Conditions

All turbulent boundary conditions were left at their default values, with the exception of inlet and outlet conditions. All walls required the entry of a roughness height. Due to the scale of the heat exchangers, and the fact that

their scale would require very fine machining, the default value of RH = 0 was left for the walls.

For the inlet, a turbulence intensity value was input at the default of zero, and the dissipation rate was set as a function of the hydraulic diameter of the heat exchanger. At the outlet, the backflow kinetic energy was set to zero, and the dissipation rate was set as a function of the hydraulic diameter.

d. Initial Conditions

For the first iteration, a turbulence intensity value of zero was entered, and the dissipation rate was again set as a function of hydraulic diameter.

3. Boiling Testing

The boiling tests were executed similarly to the original laminar tests, except the water entered at a temperature of 370 K, and the heat exchanger walls were at an initial temperature of 400 K.

a. Problem Type

The two-fluid simulation tab was selected, allowing for the phase change and transition from fluid to gas.

b. Model Options

The ‘Fluid2’ menu allows for the selection of the two-fluid simulation method. As the boiling of a fluid involves a phase change, the Enthalpy Method of calculation is selected, and the phase change sub-menu activated. The saturation temperature and latent heat are left at their default values for water.

c. Volume Conditions

Fluid one was set as saturated steam at 373 K and 101.325 kPa. The density, dynamic viscosity, specific heat, and Prandtl number were all set as constants evaluated at 373 K. Fluid two was set as water at 370 K, with density, viscosity, specific heat, and conductivity all set as constants evaluated at that temperature.

d. Boundary Conditions

For the inlet, the volume fraction of fluid two (liquid water) was set to one, and the inlet temperature ranged from 360 to 370 K.

For the outlet, the volume fraction of fluid one (steam) was set to zero, and the backflow temperature ranged from 360 to 370 K.

The walls of the heat exchanger were set to a constant temperature within the range of 380 to 400 K.

e. Initial Conditions

For the first iteration, the volume fraction of fluid two (liquid water) was set to one.

THIS PAGE INTENTIONALLY LEFT BLANK

III. NUMERICAL RESULTS

A. WATER TESTS

1. Heat Exchanger 3

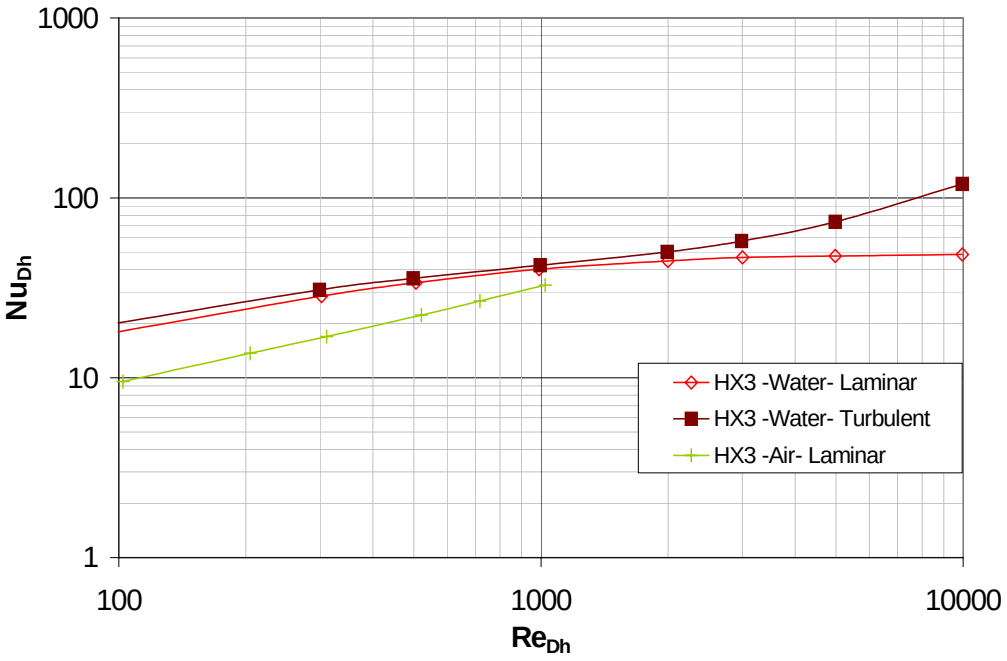

Figure 6. Nusselt number results for water flow, HX3

The water tests for heat exchanger three, shown in Figure 6, depict the desired and expected trends in Nusselt number. These results also show a definite laminar to turbulent transition zone. The laminar and turbulent numerical results are similar in magnitude until the Reynold's number of the flow reaches a value of 2000, after which the turbulent Nusselt number is much greater than the laminar value. This rapid increase not only illustrates the point of transition, but also the increased heat transfer rate which comes from turbulent mixing effects.

2. Heat Exchanger 7

The water tests for heat exchanger seven were not as conclusive as those for heat exchanger three, as many of the simulations did not converge. This can be attributed to the volume density of the model, which made the numerical calculations difficult.

The laminar tests for heat exchanger seven are inconclusive at best, especially over the transition range – see Figure 7. The Nusselt number values for Reynolds numbers of 1000, 2000, and 3000 are relatively inaccurate. Several attempts were made to get these values to converge, mainly through altering the solver controls; the values attained, while still not accurate, are more accurate than in the first round of simulations. The remaining laminar tests converged well.

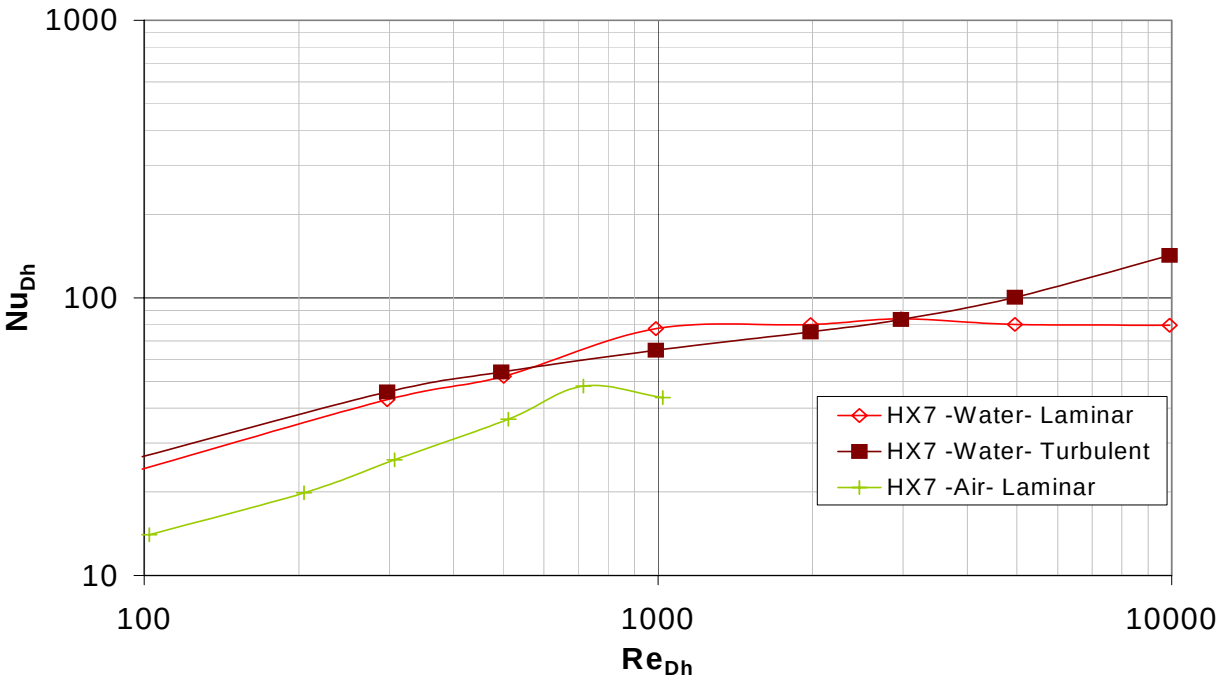

Figure 7. Nusselt number results for water flow, HX7

The turbulent tests converged well, and displayed the expected trend of much greater heat transfer at the higher Reynolds numbers. Unfortunately, due to the inaccuracies of the laminar tests, it is impossible to pin-point a definite transition range for this model.

3. Heat Exchanger 9

The water tests for heat exchanger nine converged better than those for heat exchanger seven, as it was a less dense model. However, the results are somewhat ambiguous on the transition to turbulent flow. As shown in Figure 8, the data for the laminar and turbulent tests parallel each other; there is no definitive point where the turbulent data breaks away from the laminar data. The turbulent tests show a small increase at a Reynolds number of 10000, hinting at the beginning of transition. This may imply a higher transition Reynolds number for this geometry.

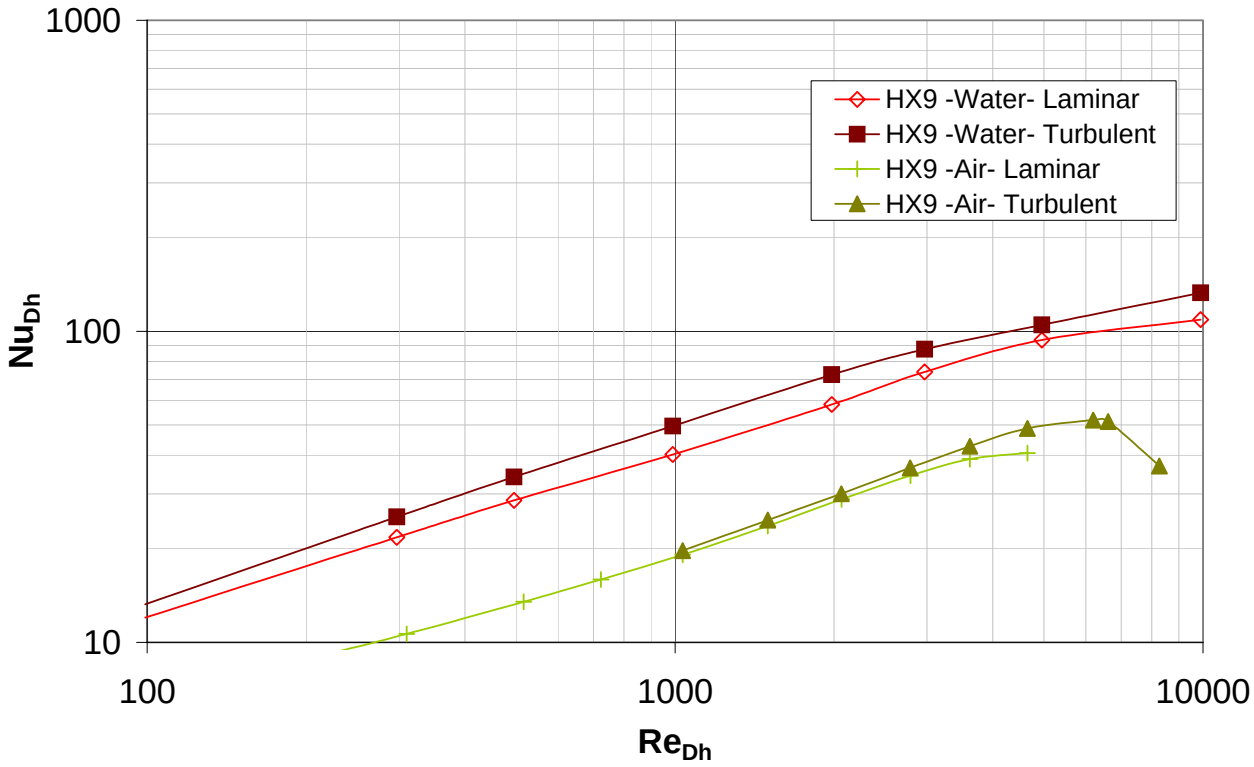

Figure 8. Nusselt number results for water flow, HX9

B. BOILING SIMULATION TESTS

The numerical simulations of boiling show a dramatic decrease in heat exchanger performance at lower Reynolds numbers. As seen in Figure 9, the steam heat transfer rate is significantly below that of liquid water by an average of an order of magnitude. As the Reynolds number approaches 10000, the heat transfer rate approaches that of liquid water.

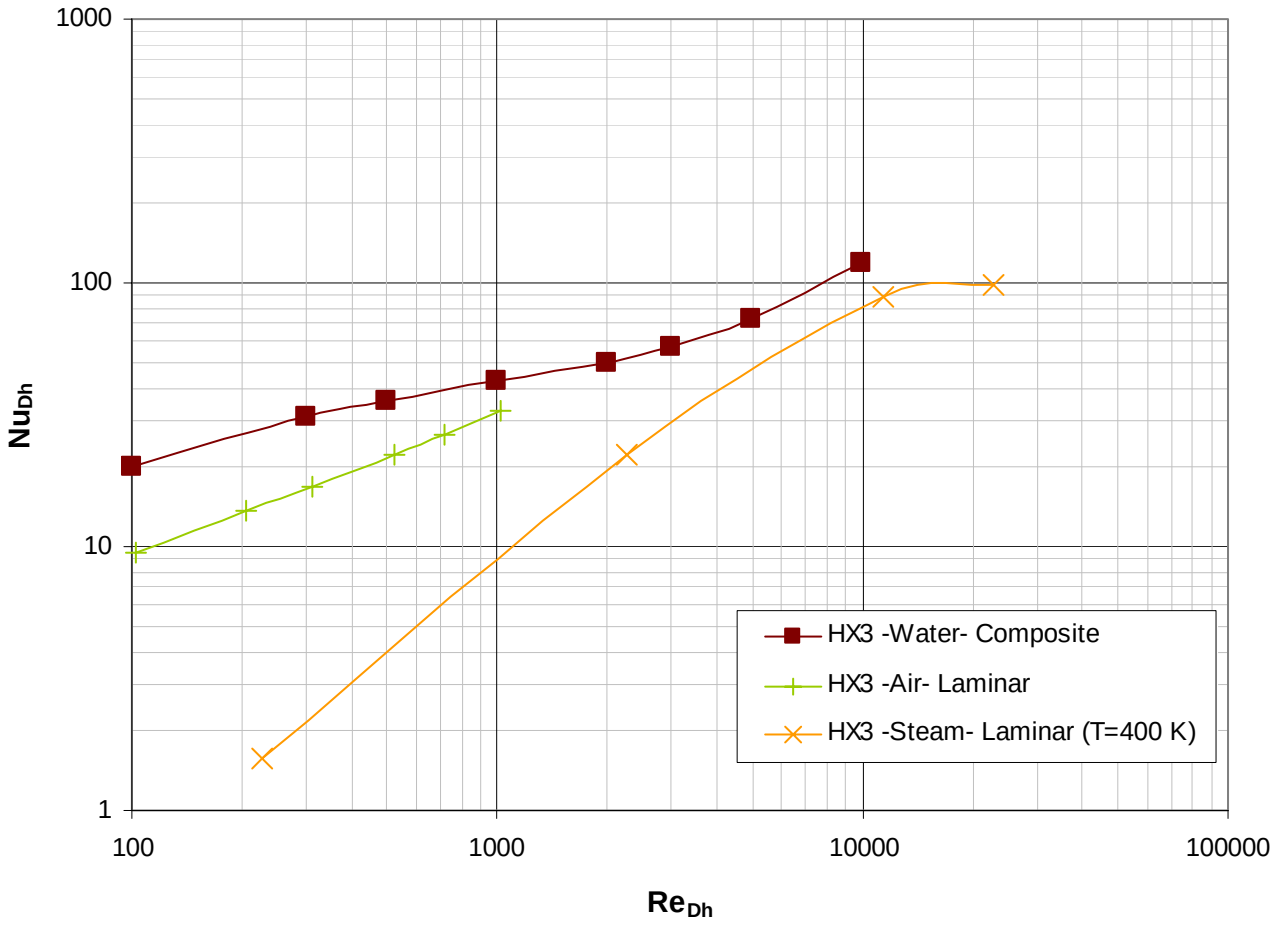

Figure 9. Nusselt number comparisons for boiling, HX3

Nusselt number is not the best measure of heat exchanger performance when there is phase change of the working fluid, due to the changing properties of the fluid. A better measure is the actual heat removal within the heat

exchanger. At lower Reynolds numbers, the blockage effects caused by the rapid expansion of steam overpowers any positive effects gained from the phase change of the fluid. However, at higher Reynolds numbers, the phase change happens more gradually, and contributes to the heat removal process.

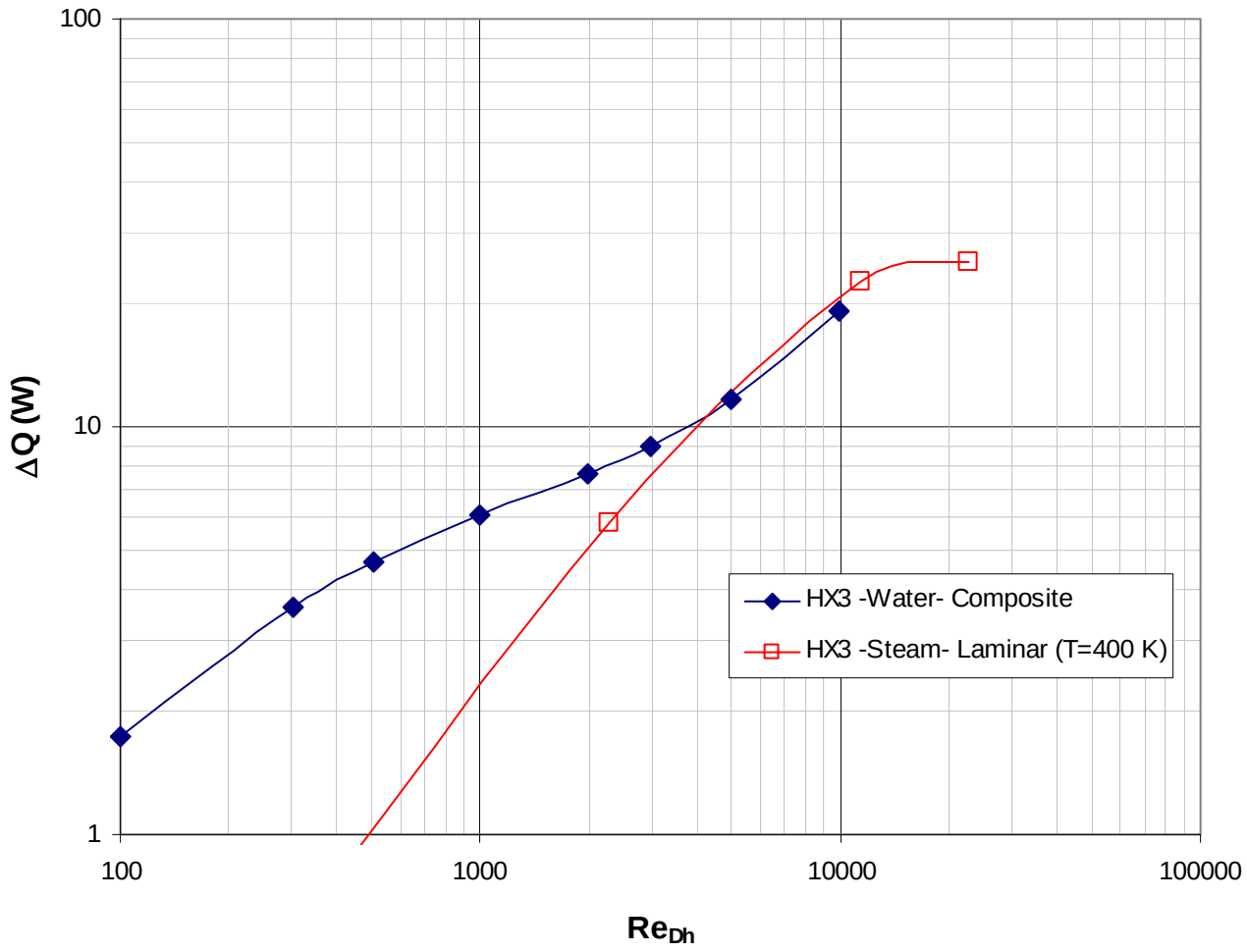

Figure 10. Heat removal comparisons for boiling, HX3

As seen in Figure 10, after a Reynolds number of 4000, the effects of phase change of the working fluid overcome the negative effects of expansion and blockage, and the heat removal rate surpasses that of purely liquid water.

The low Reynolds number results can be attributed to the high wall and fluid temperatures at the onset of the problem, and the speed of the flow for a given simulation. At lower speeds, there is more time for the wall to transfer energy to the flow, and therefore, the flow changes phase quickly. Furthermore, as the flow changes from liquid to gaseous phase, the rapid decrease in density and expansion in volume forced caused large amounts of recirculation. In some cases, this counter-flow was enough to block subsequent water flow, resulting in a very low heat transfer rate.

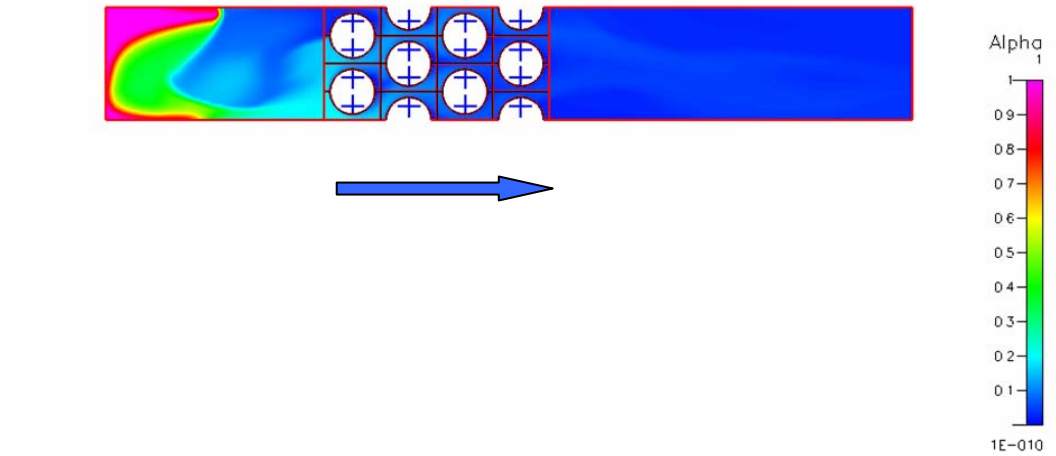

Figure 11. Phase volume fraction of flow, HX3, low Reynolds number

Figure 11 shows the effects of the rapid phase change at low Reynolds number, on the order of 10^2. The measure Alpha is the volume of liquid water over the total volume of water in the heat exchanger. At the inlet, Alpha is equal to one, corresponding to total liquid water flow. Since the entrance length prior to the pin-fins was simulated as adiabatic, heat transfer did not occur until the flow entered the pin-fin region. However, it can be seen that the Alpha value of the flow prior to the pin-fin region is almost zero, corresponding to nearly complete steam flow. This can be attributed to the rapid expansion of the water as it changed phase, and the recirculation it caused. This also illustrates the cause of the greatly decreased heat transfer rate.

The high Reynolds number results can be attributed to the higher velocity of the flow in these cases. The speed of the flow allowed less time for energy transfer from the wall to the fluid, resulting in less of the flow changing to steam. The smaller amount of expansion caused negligible recirculation, resulting in an overall a higher rate of heat transfer, as the phase change was able to contribute its full effect towards increasing the heat transfer rate.

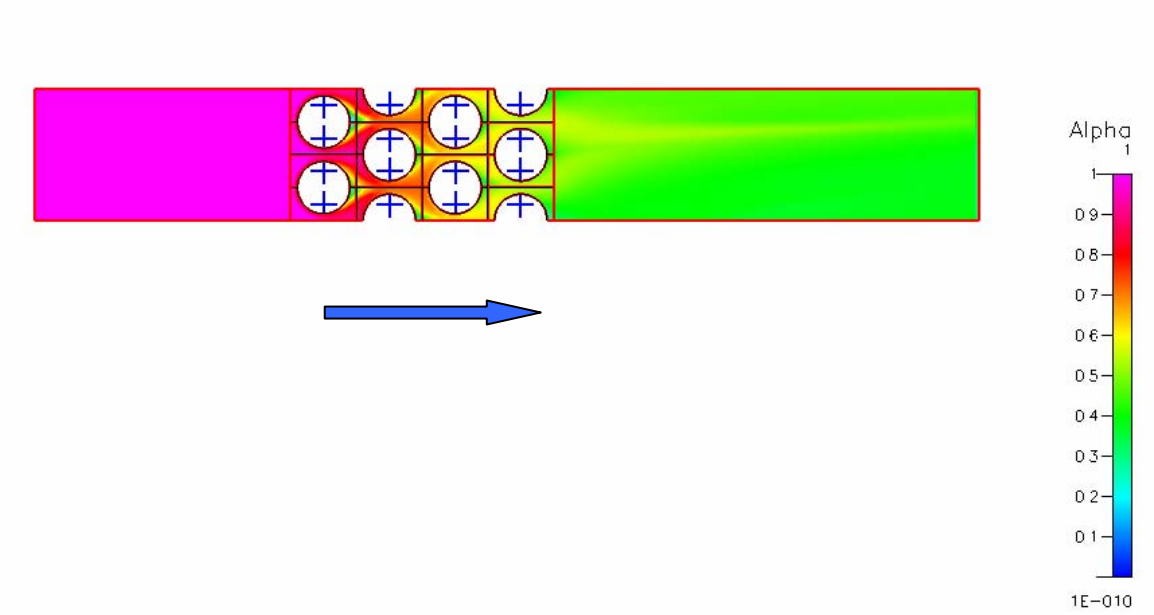

Figure 12. Phase volume fraction of flow, HX3, high Reynolds number

Figure 12 shows the volume fraction of the flow at a high Reynolds number, on the order of 10^4. The flow is completely liquid water over the adiabatic entry length, showing that there was no recirculation due to expansion. Furthermore, the flow is never completely gaseous water; the alpha over the exit length never decreases below 30 percent. This corresponds to 70 percent of the flow existing as steam.

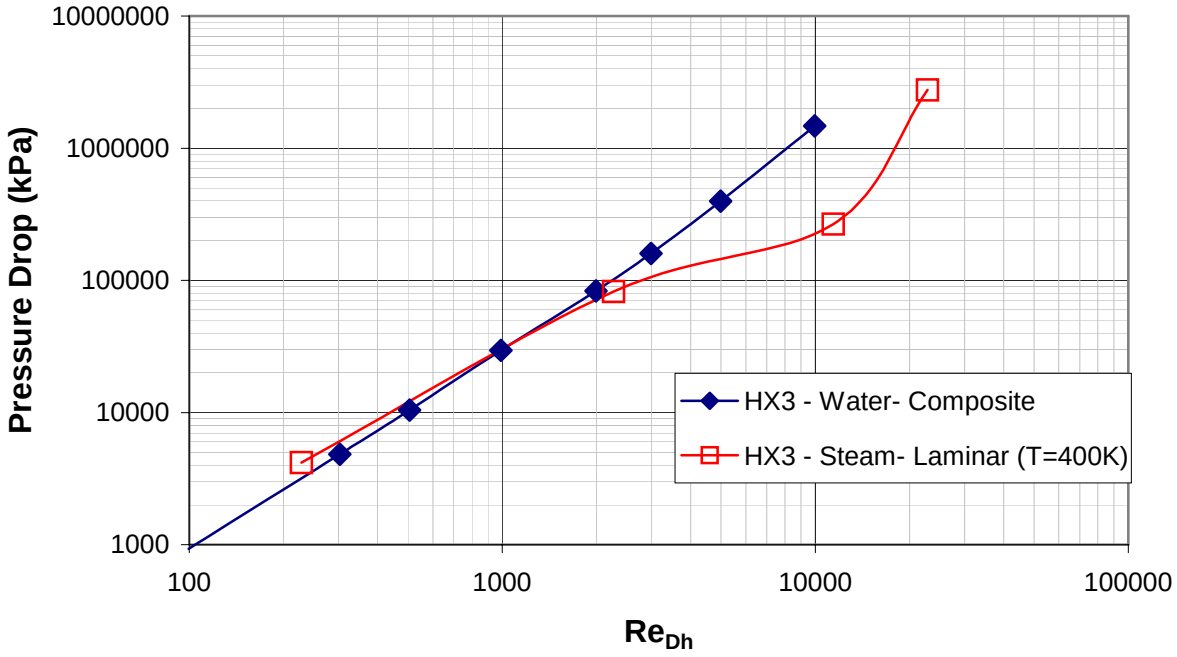

Figure 13. Phase change effects on pressure drop, HX3

Another place where the effects of the phase change were evident was in the pressure drop across the heat exchanger. The rapid expansion effects led to an increase in fluid pressure, but this increase was negligible when compared to the decrease that came from moving from the liquid to solid phase.

As it can be seen in Figure 13, pressure drop for the phase change is consistent with that of purely liquid water flow until a Reynolds number of about 1000, when the pressure drop decreases rapidly. Again, this effect can be attributed to the lower pressure of water in the gaseous phase.

C. FUEL TESTS

1. Heat Exchanger 3

The fuel tests for heat exchanger three, shown in Figure 14, depict the same trend as the water tests; transition occurs within the same range of Reynolds numbers. The laminar Nusselt numbers rise steadily in value before leveling off around a Reynolds number of 2000. The turbulent values steadily increase after a Reynolds number of 2000.

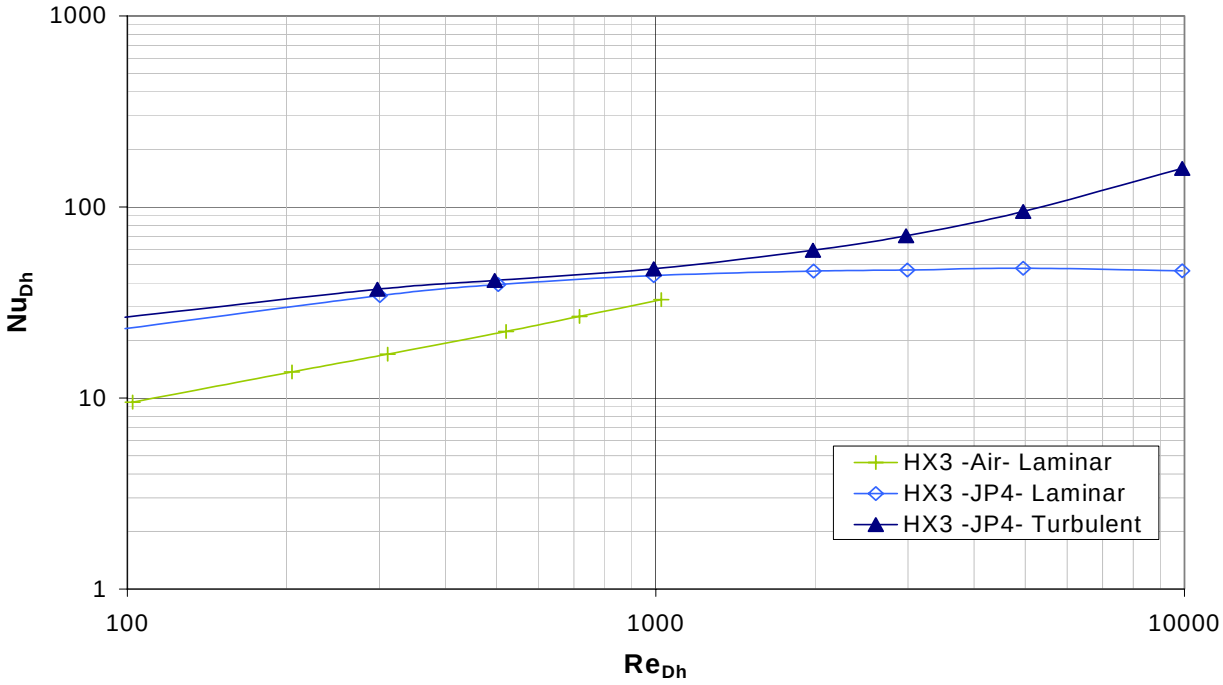

Figure 14. Nusselt number results for fuel flow, HX3

2. Heat Exchanger 7

The fuel tests for heat exchanger seven follow the same trends as the water tests (as shown in Figure 15): the laminar simulations did not converge well, but the turbulent simulations did. While it is possible to estimate the transition point using a reasonable amount of "engineering intuition," a definite range of transition values was not furnished due to the lack of useful laminar data over that Reynolds number range.

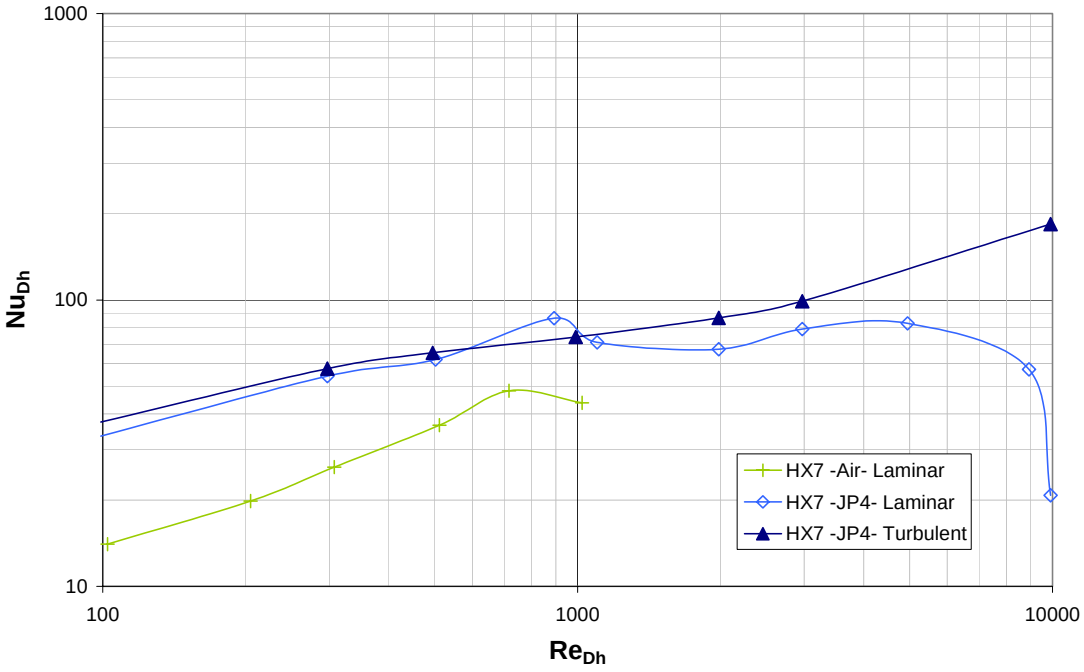

Figure 15. Nusselt number results for fuel flow, HX7

3. Heat Exchanger 9

The fuel tests for heat exchanger nine follow the same trends as those for heat exchanger three. As shown in Figure 16, both laminar and turbulent cases steadily increase with increasing Reynolds number. The breakaway point for the turbulent curve, representing the possible transition point from laminar to turbulent flow, occurs approximately at a Reynolds number of 5000. It is interesting because it corresponds with Dimas' data, which shows a transition point corresponding to a Reynolds number of 3500.

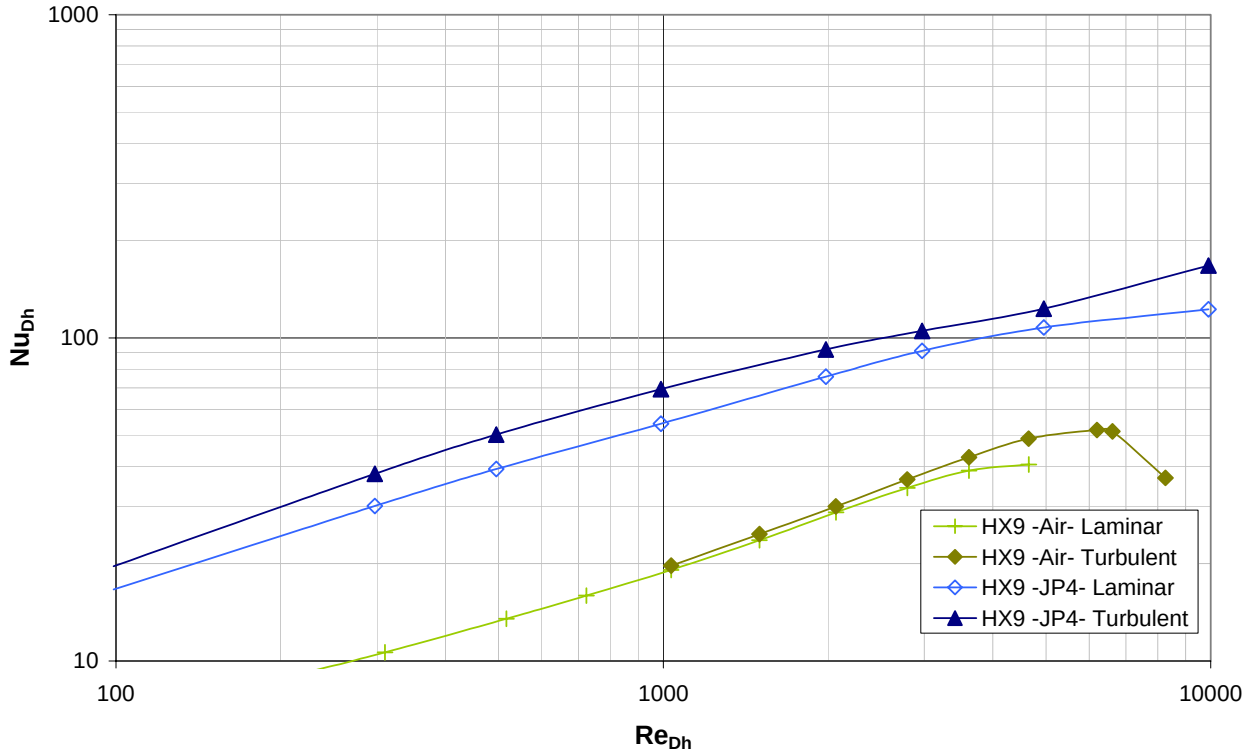

Figure 16. Nusselt number results for fuel flow, HX9

D. VALIDATION OF NUMERICAL TESTS

The effectiveness-NTU method was used to verify the accuracy of the numerical simulations performed for this study. Each data point was plotted against the theoretical relation between effectiveness and the number of transfer units. Generally, the numerical tests match well with the theoretical line, with a few outliers as discussed below.

1. Heat Exchanger 3

Heat exchanger three corroborated well with heat transfer theory. Figure 17 shows that the data points for the water and fuel tests (as well as Dimas' air tests) all fall on the theoretical line. These tests converged well, and the residuals from these tests were small enough to be negligible.

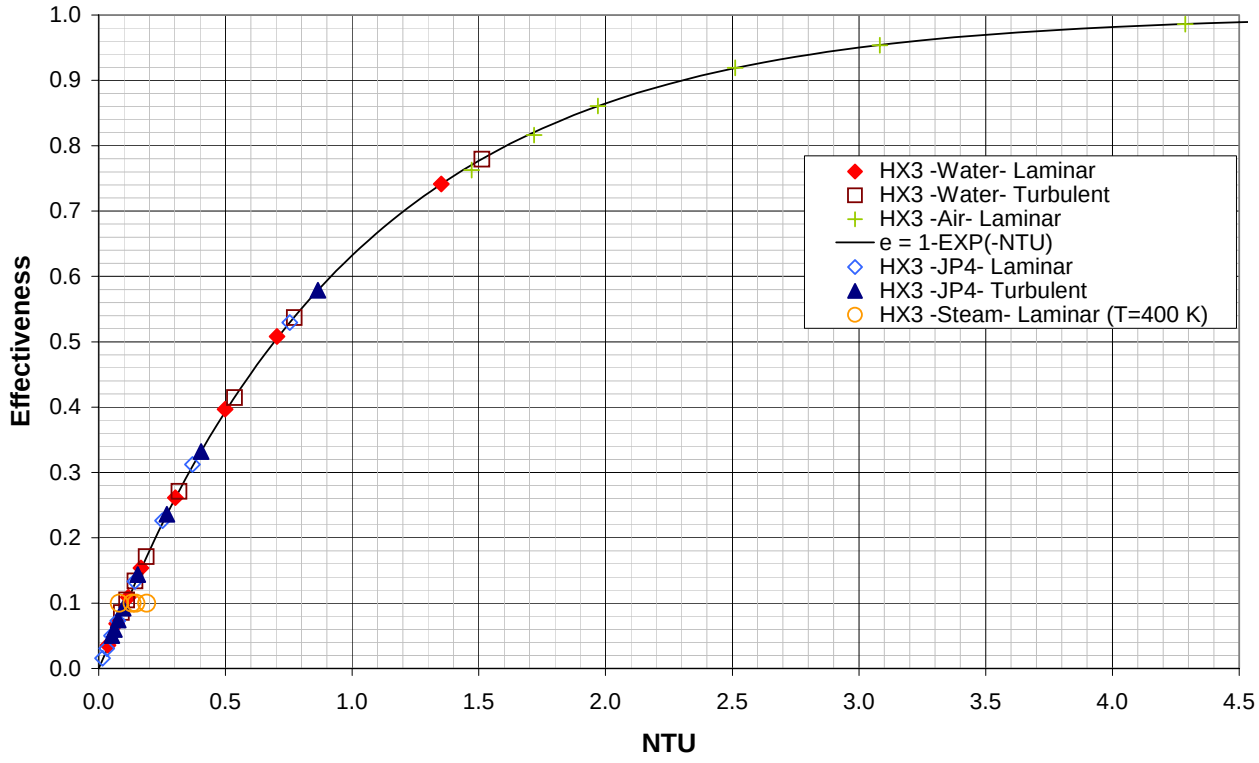

Figure 17. Effectiveness-NTU plot, HX3

The steam tests did not match up to the theoretical line as well. This can be attributed to the high heat transfer residuals in these simulations; they did not converge as well because of the use of a two-fluid model.

2. Heat Exchanger 7

Heat exchanger seven was the most troublesome of the models run in this study, and the effectiveness versus number of transfer units plot reflects this. The laminar water and fuel data points are somewhat scattered around the theoretical line for lower values of efficiency. This was expected, as these simulations did not converge well. The residuals, while not overly large, provided enough inaccuracy to incur a small amount of error.

Figure 18 shows that the turbulent water and fuel data points fall on the theoretical line, as was expected. The residuals from these simulations were small enough to be negligible.

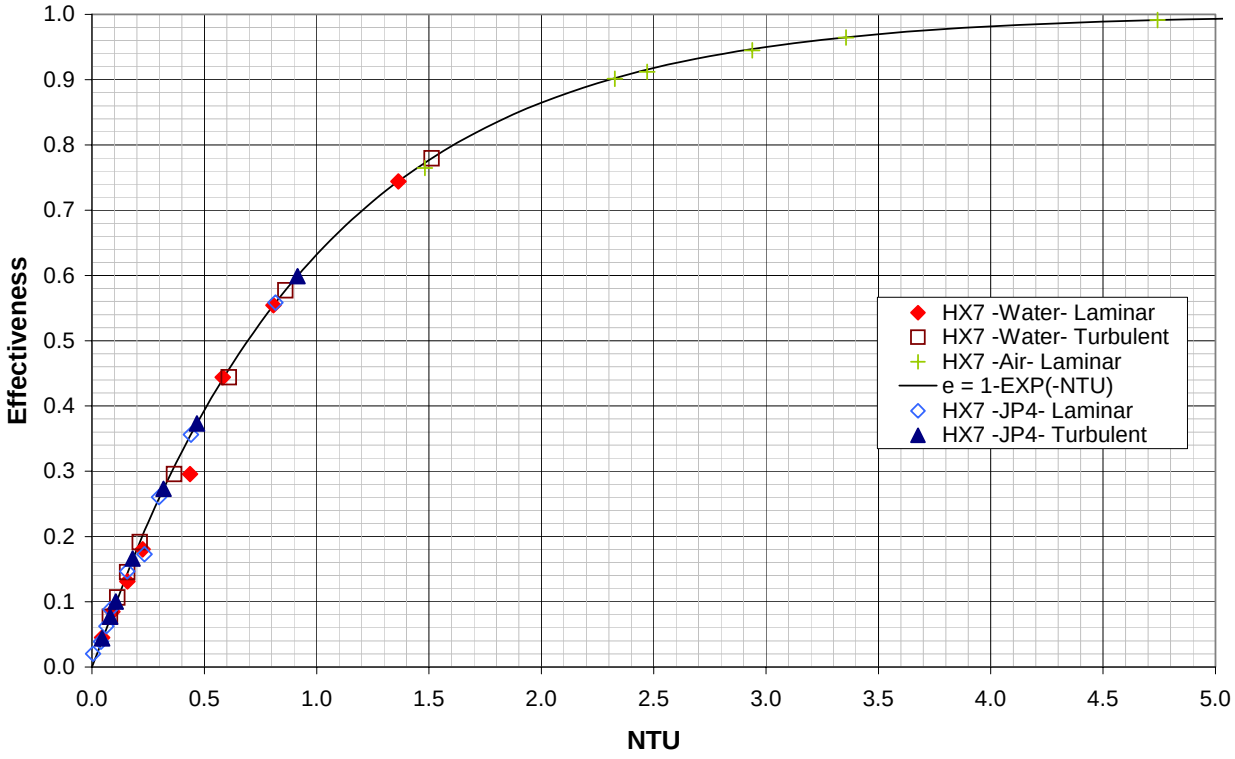

Figure 18. Effectiveness-NTU plot, HX7

3. Heat Exchanger 9

Heat exchanger nine performed well, with all data points from the laminar and turbulent fuel and water tests corroborating well with the theoretical effectiveness curve (as shown in Figure 19). This was expected, as all simulations using this model converged well, with negligible residuals.

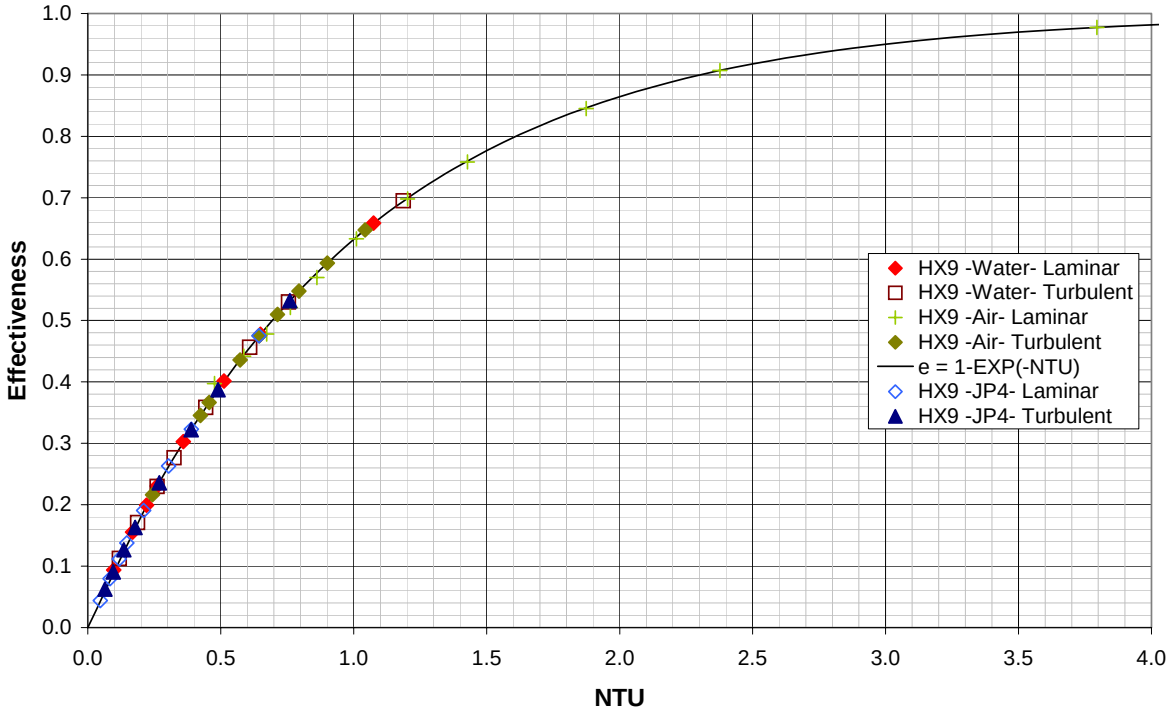

Figure 19. Effectiveness-NTU plot, HX9

IV. ANALYSIS AND DISCUSSION

A. ANALYSIS OF OBJECTIVES

1. Laminar to Turbulent Transition

The Reynolds number range for transition from laminar to turbulent flow was proven with reasonable accuracy for heat exchanger three. From the Nusselt number plots, it can be seen that the turbulent simulations begin to diverge from the laminar line between Reynolds numbers of 1000 and 2000.

Tables 3 and 4 show the percent differences between the Nusselt numbers for the laminar and turbulent simulations. For both the water and fuel tests, the differences tend to be small values (on the order of 1 to 10%) until a Reynolds number of 2000, after which they increase rapidly.

Re_{Dh} (Input)	99.63	302.38	505.95	990.61	1998.54	3001.44	4980.25	9960.46
Nu_{Dh} (Laminar)	18.02	28.46	33.79	40.13	44.59	46.69	47.53	48.54
Nu_{Dh} (Turbulent)	20.16	30.85	35.71	42.19	50.07	57.58	73.65	119.61
% Difference in Nu_{Dh}	11.84	8.40	5.69	5.14	12.30	23.34	54.94	146.40

Table 3. Percent difference between laminar and turbulent simulation Nusselt numbers; water, HX3

Re_{Dh} (Input)	99.06	300.58	503.14	990.62	1987.56	2989.75	4953.12	9906.21
Nu_{Dh} (Laminar)	23.09	34.41	39.27	43.74	46.19	46.82	47.81	46.28
Nu_{Dh} (Turbulent)	26.50	37.08	41.25	47.40	59.33	70.67	94.71	159.03
% Difference in Nu_{Dh}	14.77	7.78	5.03	8.39	28.43	50.96	98.10	243.60

Table 4. Percent difference between laminar and turbulent simulation Nusselt number; fuel, HX3

The transition range for heat exchanger seven was not proven as well as that for heat exchanger three. This is mainly due to the fact that the laminar simulations tended to diverge starting around a Reynolds number of 1000. The lack of good laminar data to compare with the turbulent data in that range makes it hard to pin-point the transition. However, it is possible to say that the divergence in the laminar simulations was caused by the fact that the flow should

have been modeled as turbulent flow, and the numerical process was breaking down without the inclusion of turbulent effects.

From Table 5, it can be seen that the flow is turbulent at a Reynolds number of 5000, but it is impossible to tell at which point before that number the flow becomes turbulent (see also Table 6).

Re_{Dh} (Input)	99.1	297.2	501.1	990.7	1981.4	2972.1	4953.5	9907.0
Nu_{Dh} (Laminar)	24.19	42.97	52.21	77.43	80.15	83.98	80.30	79.72
Nu_{Dh} (Turbulent)	26.80	45.82	54.04	64.78	75.34	83.49	100.43	142.15
% Difference in Nu_{Dh}	10.82	6.62	3.51	-16.34	-6.00	-0.59	25.07	78.31

Table 5. Percent difference between laminar and turbulent simulation Nusselt number; water, HX7

Re_{Dh} (Input)	99.1	297.2	495.4	990.7	1981.4	2972.1	9907.0
Nu_{Dh} (Laminar)	33.48	54.14	61.93	25.18	67.27	79.09	20.77
Nu_{Dh} (Turbulent)	37.48	57.52	65.38	74.20	86.66	98.98	183.97
% Difference in Nu_{Dh}	11.94	6.25	5.57	194.64	28.83	25.14	785.66

Table 6. Percent difference between laminar and turbulent simulation Nusselt number; fuel, HX7

It is difficult to predict the transition zone from the heat exchanger nine data, as the turbulent simulation Nusselt number curves follows the laminar simulation curves very closely, and there is no clear point where they diverge. Since transition can occur over a wide range of Reynolds numbers for internal flow, it may be safe to assume that the transition zone is higher than 10^4 for this geometry.

Tables 7 and 8 show the percent differences between the laminar and turbulent tests for heat exchanger nine. Note that the difference is nearly constant, or on the same order, for all the Reynolds numbers, and no clear transition zone can be seen.

Re_{Dh} (Input)	99.1	297.1	495.3	990.5	1981.0	2971.4	4952.4	9904.8
Nu_{Dh} (Laminar)	12.00	21.76	28.62	40.15	58.22	73.98	93.83	109.10
Nu_{Dh} (Turbulent)	13.26	25.30	34.01	49.59	72.52	87.57	104.84	132.98
% Difference in Nu_{Dh}	10.44	16.28	18.81	23.53	24.55	18.36	11.74	21.89

Table 7. Percent difference between laminar and turbulent simulation Nusselt number; water, HX9

Re_{Dh} (Input)	99.0	297.2	495.2	990.5	1981.0	2971.4	4952.4	9904.8
Nu_{Dh} (Laminar)	16.64	30.16	39.25	54.22	75.82	91.18	107.71	122.53
Nu_{Dh} (Turbulent)	19.62	37.95	50.19	69.39	92.06	105.01	123.13	167.41
% Difference in Nu_{Dh}	17.92	25.83	27.86	27.98	21.42	15.17	14.31	36.63

Table 8. Percent difference between laminar and turbulent simulation Nusselt number; fuel, HX9

Since the laminar to turbulent breakaway point occurs over a wide range of Reynolds numbers for the three different geometries, it is safe to assume that there is no predetermined switch in CFD-ACE that automatically activates turbulence at a certain Reynolds number.

It is possible to conclude that CFD-ACE can be used to find and predict the laminar to turbulent transition zone for different geometries by comparing the data from laminar and turbulent simulations.

2. Advantages of Water over Air

The advantages of water over air as a working are readily apparent from the Nusselt number plots from the previous chapter, which showed that water had higher Nusselt numbers than air for corresponding Reynolds numbers. The increase in Nusselt number depended upon Reynold's number, and generally decreased as Reynolds number increased. Tabulated below (Tables 9-11) are some typical results for each heat exchanger. Note that heat exchanger nine has a wider range of values, as Dimas worked in the turbulent range with that model.

Re_{Dh} (Input)	100	500	1000
Nu_{Dh} (Air)	9.53	22.28	32.72
Nu_{Dh} (Water)	18.02	33.79	40.13
% Difference in Nu_{Dh}	**89.09**	**51.66**	**22.63**

Table 9. Percent increase in Nusselt number for water as compared to air, HX3

Re_{Dh} (Input)	100	500	1000
Nu_{Dh} (Air)	14.02	36.53	43.72
Nu_{Dh} (Water)	26.80	54.04	64.78
% Difference in Nu_{Dh}	**91.16**	**47.93**	**48.17**

Table 10. Percent increase in Nusselt number for water as compared to air, HX7

Re_{Dh} (Input)	100	500	1000	5000
Nu_{Dh} (Air)	7.18	13.51	19.11	48.74
Nu_{Dh} (Water)	12.00	28.62	40.15	104.84
% Difference in Nu_{Dh}	**67.19**	**111.93**	**110.04**	**115.10**

Table 11. Percent increase in Nusselt number for water as compared to air, HX9

Further evidence of the increase in heat removal rate comes from a comparison of the heat transfer coefficients (Tables 12-14).

Re_{Dh} (Input)	100	500	1000
$h_{array,ave}$ (Air) (W/m^2*K)	834.01	1949.46	2863.53
$h_{array,ave}$ (Water) (W/m^2*K)	36890.91	69163.06	82144.75
% Difference in $h_{array,ave}$	**4323.33**	**3447.81**	**2768.65**

Table 12. Percent increase in heat transfer coefficient for water as compared to air, HX3

Re_{Dh} (Input)	100	500	1000
$h_{array,ave}$ (Air) (W/m^2*K)	2767.40	7209.69	8627.98
$h_{array,ave}$ (Water) (W/m^2*K)	110994.56	239566.77	355295.18
% Difference in $h_{array,ave}$	**3910.79**	**3222.84**	**4017.94**

Table 13. Percent increase in heat transfer coefficient for water as compared to air, HX7

Re_{Dh} (Input)	100	500	1000	5000
$h_{array,ave}$ (Air) (W/m^2*K)	246.00	462.70	654.87	1669.91
$h_{array,ave}$ (Water) (W/m^2*K)	9717.31	23167.81	32495.96	84864.78
% Difference in $h_{array,ave}$	**3850.05**	**4907.10**	**4862.24**	**4982.01**

Table 14. Percent increase in heat transfer coefficient for water as compared to air, HX9

From the effectiveness plots, it is evident that using water as a working fluid offers much lower values of heat exchanger effectiveness and number of transfer units for the corresponding Reynolds numbers. Generally, both effectiveness and the number of transfer units decreased as Reynolds number increased. Tabulated below (Tables 15-17) are some typical results for each heat exchanger. Note that again, there are more values for heat exchanger nine, as Dimas worked in the turbulent range.

Re_{Dh} (Input)	100	500	1000
ε (Air)	0.9863	0.8606	0.7625
ε (Water)	0.7413	0.3970	0.2613
% Difference in ε	-24.83	-53.87	-65.74
NTU (Air)	4.2877	1.9700	1.4721
NTU (Water)	1.3519	0.4991	0.3028
% Difference in NTU	-68.47	-74.66	-79.43

Table 15. Percent decrease in effectiveness and NTU for water as compared to air, HX3

Re_{Dh} (Input)	100	500	1000
ε (Air)	0.9912	0.9121	0.7648
ε (Water)	0.7795	0.4440	0.2956
% Difference in ε	-21.37	-51.32	-61.35
NTU (Air)	4.7421	2.4714	1.4813
NTU (Water)	1.5112	0.6093	0.3652
% Difference in NTU	-68.13	-75.35	-75.35

Table 16. Percent decrease in effectiveness and NTU for water as compared to air, HX7

Re_{Dh} (Input)	100	500	1000	5000
ε (Air)	0.97750	0.75842	0.63317	0.43596
ε (Water)	0.65873	0.40136	0.30271	0.17091
% Difference in ε	-32.61	-47.08	-52.19	-60.80
NTU (Air)	3.7947	1.4275	1.0102	0.5726
NTU (Water)	1.0746	0.5124	0.3594	0.1877
% Difference in NTU	-71.68	-64.10	-64.42	-67.22

Table 17. Percent decrease in effectiveness and NTU for water as compared to air, HX9

3. Advantages of Fuel over Air

The use of fuel as a working fluid again offered a large increase in the value of Nusselt number when compared to air results for the same Reynolds number. Again, the increase in Nusselt number depended upon Reynolds number, and usually decreased in magnitude as Reynolds number increased. Several results from each heat exchanger are tabulated and compared below (Tables 18-20).

Re_{Dh} (Input)	100	500	1000
Nu_{Dh} (Air)	9.53	22.28	32.72
Nu_{Dh} (Fuel)	23.09	39.27	43.74
% Difference in Nu_{Dh}	**142.26**	**76.30**	**33.66**

Table 18. Percent increase in Nusselt number for fuel as compared to air, HX3

Re_{Dh} (Input)	100	500	1000
Nu_{Dh} (Air)	14.02	36.53	43.72
Nu_{Dh} (Fuel)	37.48	65.38	74.20
% Difference in Nu_{Dh}	**167.31**	**78.96**	**69.72**

Table 19. Percent increase in Nusselt number for fuel as compared to air, HX7

Re_{Dh} (Input)	100	500	1000	5000
Nu_{Dh} (Air)	7.18	13.51	19.11	48.74
Nu_{Dh} (Fuel)	16.64	39.25	54.22	123.13
% Difference in Nu_{Dh}	**131.72**	**190.65**	**183.65**	**152.62**

Table 20. Percent increase in Nusselt number for fuel as compared to air, HX9

Further evidence of the increase in heat removal rate comes from a comparison of the heat transfer coefficients (Tables 21-23).

Re_{Dh} (Input)	100	500	1000
$h_{array,ave}$ (Air) (W/m^2*K)	834.01	1949.46	2863.53
$h_{array,ave}$ (Fuel) (W/m^2*K)	9813.49	16692.45	18589.23
% Difference in $h_{array,ave}$	**1076.67**	**756.26**	**549.17**

Table 21. Percent increase in heat transfer coefficient for fuel as compared to air, HX3

Re_{Dh} (Input)	100	500	1000
$h_{array,ave}$ (Air)	2767.40	7209.69	8627.98
$h_{array,ave}$ (Fuel)	31902.60	59004.54	23993.47
% Difference in $h_{array,ave}$	**1052.80**	**718.41**	**178.09**

Table 22. Percent increase in heat transfer coefficient for fuel as compared to air, HX7

Re_{Dh} (Input)	100	500	1000	5000
$h_{array,ave}$ (Air) (W/m^2*K)	246.00	462.70	654.87	1669.91
$h_{array,ave}$ (Fuel) (W/m^2*K)	2796.27	6597.04	9112.02	20693.14
% Difference in $h_{array,ave}$	**1036.67**	**1325.77**	**1291.43**	**1139.18**

Table 23. Percent increase in heat transfer coefficient for fuel as compared to air, HX9

From the effectiveness plots, it can be shown that using fuel as a working fluid offers much smaller values of heat exchanger effectiveness and number of transfer units for the corresponding Reynolds numbers. Generally, both effectiveness and the number of transfer units decreased as Reynolds number increased. Tabulated below are some typical results for each heat exchanger (Tables 24-26).

Re_{Dh} (Input)	100	500	1000
ε (Air)	0.9912	0.9121	0.7648
ε (Fuel)	0.5990	0.2730	0.1661
% Difference in ε	**-39.57**	**-70.06**	**-78.29**
NTU (Air)	4.7421	2.4714	1.4813
NTU (Fuel)	0.9142	0.3189	0.1809
% Difference in NTU	**-80.72**	**-87.10**	**-87.78**

Table 24. Percent decrease in effectiveness and NTU for fuel as compared to air, HX3

Re_{Dh} (Input)	100	500	1000
ε (Air)	0.9863	0.8606	0.7625
ε (Fuel)	0.5295	0.2262	0.1332
% Difference in ε	-46.31	-73.71	-82.53
NTU (Air)	4.2877	1.9700	1.4721
NTU (Fuel)	0.7537	0.2524	0.1428
% Difference in NTU	-82.42	-87.19	-90.30

Table 25. Percent decrease in effectiveness and NTU for fuel as compared to air, HX7

Re_{Dh} (Input)	100	500	1000	5000
ε (Air)	0.9775	0.7584	0.6332	0.4360
ε (Fuel)	0.4752	0.2630	0.1907	0.0906
% Difference in ε	-51.39	-65.32	-69.88	-79.23
NTU (Air)	3.7947	1.4275	1.0102	0.5726
NTU (Fuel)	0.6443	0.3040	0.2100	0.0954
% Difference in NTU	-83.02	-78.70	-79.22	-83.35

Table 26. Percent decrease in effectiveness and NTU for fuel as compared to air, HX9

4. The Effect of Boiling on Heat Exchanger Performance

The boiling of fluid within the heat exchanger has an overall negative effect on system performance, when Nusselt number results are examined. This trend was very prevalent at low Reynolds numbers, in the range of 10^2 to 10^3. This was due to the blockage caused by water as it expanded from a liquid to a gas. At higher Reynolds number, the flow overcame the blockage, and used the phase change to effect greater heat transfer rates, though still not as high as those of water at the same Reynolds numbers. Table 27 shows several examples of these trends.

Re_{Dh} (Input)	500	1000	5000	10000
Nu_{Dh} (Water)	33.79	40.13	94.71	159.03
Nu_{Dh} (Steam)	4.0	9.0	47.8	81.0
% Difference in Nu_{Dh}	-88.16	-77.57	-49.52	-49.07

Table 27. Decrease in Nusselt number due to boiling, HX3

However, a different trend emerges when the heat removal from the system is examined. The latent heat removal that occurs during a phase change is extremely prevalent at higher Reynolds numbers (over 10^3). Again, this is due to the fact that at lower Reynolds numbers, blockage of the flow trumped any positive effects on heat transfer from the phase change. Table 28 shows several examples of this trend.

Re_{Dh} (Input)	1000	2000	3000	5000	10000
ΔQ (W) (Water)	5.81	7.66	9.00	11.70	19.20
ΔQ (W) (Steam)	1.2	5.1	7.7	12.0	21.0
% Difference in (ΔQ)	-79.35	-33.42	-14.44	2.56	9.38

Table 28. Increase in heat removal due to boiling, HX3

From these results, it is safe to conclude that if boiling of fluid within a system is probable, then it is beneficial to run the flow at a higher Reynolds number to avoid the drastic decreases in heat transfer rate that occur at low velocities, and to take full advantage of the positive effect of the phase change. Furthermore, one can also conclude that Nusselt number is not the most accurate way to measure the effect of phase change in a system, due to the changing nature of the fluid properties.

THIS PAGE INTENTIONALLY LEFT BLANK

V. CONCLUSIONS AND RECOMMENDATIONS

Water and fuel offered much greater heat transfer coefficients than air for the same Reynolds numbers. For water, the heat transfer coefficient was in the range of 10,000 to 360,000 W/m^2*K for Reynolds numbers between 100 and 10000. For fuel, the heat transfer coefficient was in the range of 3,000 to 32,000 W/m^2*K for the same range of Reynolds numbers. This is a large increase compared to air, which offered values between 250 and 9,000 W/m^2*K over the same range of Reynolds numbers.

While this fact in itself is attractive, it is important to note the corresponding decrease in heat exchanger effectiveness that occurred with the transition to water (decreased by 21 to 66 percent) and fuel (decreased by 40 to 83 percent). Also of note is the fact that effectiveness was higher at lower Reynolds numbers than it was for higher (turbulent) values (see Tables 17 and 26).

The laminar to turbulent transition zone was determined with reasonable degree of confidence to be in the range of 1500 to 2000 for one of the three heat exchanger geometries used in this study. The other geometries did not offer such conclusive data. This was mainly due to the inability to compare laminar and turbulent data for the lack of corresponding data points (due to divergence issues).

From the simulations, it can be seen that the laminar flow simulations were accurate until the commonly accepted transition range, after which the turbulent simulations gave the better values. In that range, it often became difficult to simulate the flow using a laminar model, as the solutions tended to diverge. This made the transition zone difficult to prove with absolute certainty, for lack of comparative laminar data in several cases.

Turbulent flow certainly offers a large amount of heat transfer (see Tables 3-8); that is attractive, given the small footprint of the heat exchangers used in this study.

Boiling adversely affects heat exchanger performance at lower Reynolds numbers (with decreases up to 80 percent) due to the blockage caused by rapid fluid expansion and the resulting flow patterns. At higher Reynolds numbers (entering the turbulent flow regime), it is possible to minimize the degradation of performance caused by blockage by utilizing the high heat transfer rates that occur at higher velocities (Reynolds numbers 5000-10000), and the latent heat removal that occurs during the phase change of a fluid to a gas (see Table 28). Under these conditions, it is possible to achieve an increase of up to 10 percent in the heat removal rate of the system.

Future investigations would benefit from experimental data that could corroborate the conclusions of these simulations. That data could be used to supplement the simulated results in areas where the numerical methods broke down. Also, an investigation into the transient behavior of turbulent flow would further expand upon the data collected from these steady flow simulations.

LIST OF REFERENCES

1. Choo, J.S., “Numerical Analysis of the Performance of Staggered Micro Pin-Fin Heat Exchangers,” Naval Postgraduate School, Monterey, California, 2003.

2. Dimas, S., “A CFD Analysis of the Performance of Pin-Fin Laminar Flow Micro/Meso Scale Heat Exchangers.” Naval Postgraduate School, Monterey, California, 2005.

3. Furukawa America Website http://www.furukawaamerica.com, (accessed June 03, 2006).

4. Incropera, F.P. and DeWitt, D.P. *Introduction to Heat Transfer, 4TH Ed*. New York: John Wiley and Sons, 1996.

5. Metzger, D.E., Fan, C.S., Haley, S.W., “Effects of Pin Shape and Array Orientation on Heat Transfer and Pressure Loss in Pin Fin Arrays.” *Journal of Engineering for Gas Turbines and Power*, *Vol. 106*, (1984): 252-257.

6. White, F.M. *Fluid Mechanics, 4TH Ed.* New York: McGraw-Hill, Inc., 1999.

THIS PAGE INTENTIONALLY LEFT BLANK

INITIAL DISTRIBUTION LIST

1. Defense Technical Information Center
   Ft. Belvoir, Virginia

2. Dudley Knox Library
   Naval Postgraduate School
   Monterey, California

3. Professor Ashok Gopinath
   Naval Postgraduate School
   Monterey, California

4. Professor Jose Sinibaldi
   Naval Postgraduate School
   Monterey, California

5. ENS Michael A. Sammataro, USN
   Naval Postgraduate School
   Monterey, California